CHAPTER 5

Development of Waterborne Polyurethane-urea Dispersion using Castor Oil

5.1. Introduction

Waterborne polyurethanes (WPUs) have become a focus of standard research due to their steep cost reduction and ability to manage Volatile organic compounds (VOCs) during processing. WPUs offer a wide spectrum of advantages like environmental friendliness, appreciable molecular weight, rigidity, tailored properties of the cast, controlled viscosity, and user-friendly applicability.[1–3] Manageable formulation and excellent properties make WPUs quite usable in the application sectors. Various processes like prepolymer-mixing, acetone, melt-dispersion, and ketamine-ketazine have been applied to combine the polyols and diisocyanates in order to develop designed WPUs. [4–6] In the general route of prepolymer mixing process[7], the prepolymer (hydrophilically modified) is mixed with isocyanates followed by deionized water. After that chain extension proceeded with amines in the dispersion. In the acetone process[8], acetone is chosen as a solvent in which the hydrophilically modified prepolymer and isocyanate are dissolved, chain extension is done with diamines, and finally water is added. As the adding water into the system, solvent removal initiated, resulting in pure WPU dispersion. Melt dispersion[9], ketamine-ketazine, and other processes[10] also exist, but these prepolymer mixing and acetone processes are extensively used in the synthesis of WPU dispersions.

Among various vegetable oil (VOs), castor oil (CO) offers many advantages, such as low cost and an average OH functionality of 2.7, making it best for use with isocyanate to prepare cross-linked PU. In contrast, other VO usually requires chemical modification to produce polyols for PU synthesis. Also, the long non-polar fatty acid chains of CO give the formed film softness, hydrophobicity, and flexing resistance.[11,12] Therefore, CO is a valuable raw material in PU manufacturing, with applications in paints, coatings, inks, lubricants, and many other fields.[1,13]

Madbouly et al.[14] synthesized CO-based WPUs and successfully investigated the rheology of these dispersions with the function of angular frequency, solid content, and temperature. The results provided insights into the relationships between rheological properties and PU structure, alongwith coating performance under typical conditions encountered by WPUs during use. Xuan Ji et al.[15] developed the CO-modified anionic WPUs and internal cross-linked with polydimethylsiloxane using a prepolymer mixing process. These anionic WPU films exhibited good resistance against solvent and water, better thermal stability, and mechanical strength and found promising environmentally friendly materials for decorative and protective coatings. Milena Špirková et al.[16] synthesized CO-based WPU-

urea/silica nanocomposites to enhance the mechanical strength of the PU films. Chaoqun Zhang et al.[1] also synthesized CO-based WPUs and systematically investigated their good tensile strength and excellent self-healing efficiency. Also, the broad Tg of the PU endowed the developed films with an excellent versatile shape-memory effect, including a dual- to quadruple-shape memory effect. Lu et al.[17] synthesized CO-based WPUs and blended them with starch to obtain a newer plastic with excellent physical properties. It was shown that these WPUs, due to the CO as the soft segment, led to gelation and higher cross-linking, which was difficult in dispersing and therefore required a large quantity of solvent to dilute the prepolymer. Qu and Chen[18] synthesized both CO-based WPUs and CO/polypropylene glycol (PPG) mixed soft-segment WPUs and studied their coating properties to replace single-component solvent-borne PU coatings. They found good results of the synthesized CO/PPG mixed soft-segment WPUs for film-forming property and better for their applications in coating. Gurunathan et al.[19] synthesized CO-based WPU/polyaniline conducting polymer blend films and found that the thermal stability of the conducting blend films improved with the incorporation of polyaniline.

Taking into consideration the economic and environmental importance of using sustainable resource-based new materials to replace PU polymers derived from petrochemicals, we aimed to develop the newer CO-based waterborne polyurethane-urea (WPUU) for thermally and mechanically strong films for better coating applications.

In the present chapter, CO-based WPUU polymers were prepared by a prepolymer mixing process in which prepolymers were prepared using CO, IPDI, and DMPA. The prepared prepolymer was neutralized with TEA and further mixed with 1,8-diaminooctane (OA) using different concentrations of 0.1, 0.5, and 1 wt%. The synthesized WPUU polymers were characterized using DLS, electrolytic stability, and ATR-FTIR. The chemical resistance performance of the WPUU films was assessed against water, acid, alkali, salt, and organic solvents using the immersion method. The thermal stability of the synthesized WPUU films was investigated through TGA and DSC analyses. The kinetic parameters of WPUU polymers were calculated using the Kissinger method. Finally, the morphologies of the synthesized WPUU films were analyzed using SEM. The present work demonstrates that the newly synthesized WPUU films are promising for their further coating applications.

5.2. Experimental

5.2.1. Material

Dimethylolpropionic acid (DMPA) and 1,8-Octanediamine (OA) received from Sigma Aldrich India. Isophorone diisocyanate (IPDI) and triethyamine (TEA) were procured from Merck India. Methyl ethyl ketone (MEK) and dibutyltin dilaurate (DBTDL) were obtained from TCI Chemicals India.

5.2.2. Methods

5.2.2.1 Synthesis of CO-based waterborne polyurethane-urea(WPUU) dispersions

The chemical reaction of WPUUs synthesis using the CO as bioresources is shown in **Figure 5.1.** The prepolymer mixing process of such anionic WPPU synthesis has been previously reported with synthetic polyol [15,20]. The main compositions of basic components used for the WPUU formulations are given in **Table 5.1**.

CO was charged into a 500 mL four-necked RBF equipped with a mechanical stirrer, N_2 inlet, condenser, and thermometer. During stirring, the content was kept at 80°C to 90°C for 30 min, followed by adding the DBDTL (0.03 wt%) and IPDI to the homogenized mixtures. The reaction was performed at 80°C for 2 hr in an inert atmosphere. After that, DMPA dissolved in MEK was charged to the RBF. The reaction content was heated to 85°C. When the prepolymer was then cooled to 55°C, MEK was again added to dilute the prepolymer, and the neccessary TEA was charged. To neutralize the carboxylic group, stirring was kept for 45 min. A calculated amount of distilled water (70 wt%) was added dropwise under stirring. After that, OA was added for the chain extension in the reaction. The chain-extension reaction was kept to proceed at RT for 2 hr with high stirring. After the proper removal of MEK, the final WPUU dispersion with a 30% solid content was obtained.

Table 5.1. The formulation of all the synthesized CO-based WPUUs

Sample	CO (moles)	IPDI (moles)	DMPA (moles)	TEA (moles)	OA (wt %)
WPUU0	1.0	2.5	0.9	0.9	0.0
WPUU1	1.0	2.5	0.9	0.9	0.1
WPUU2	1.0	2.5	0.9	0.9	0.5
WPUU3	1.0	2.5	0.9	0.9	1.0

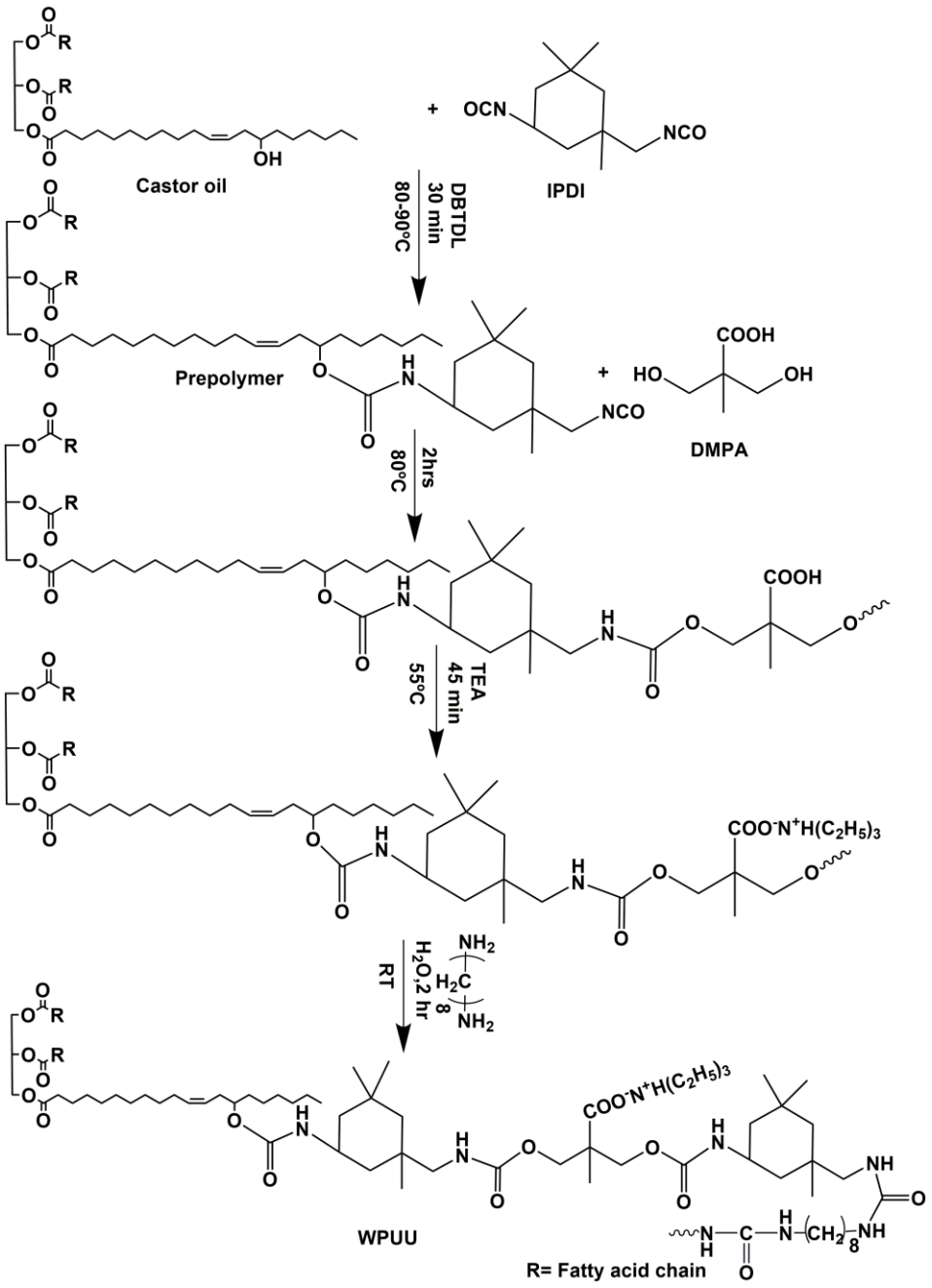

Figure 5.1. Synthesis of CO-based WPUU dispersion

5.2.2.2 Preparation of WPUU films

Freshly synthesized WPUU dispersion was casted into a silicon mold and kept at RT for almost 24 hr. After that the mold was again kept in to oven at 60°C for 8 hr for proper curing. The cured WPUU film was then stored for further studies.

5.3.3. Characterization

5.3.3.1. Physical characteristics

Physical characterizations of all the synthesized WPUU dispersions were performed to examine their dispersion stability and appearance. All samples were centrifuged at 3000

RPM for 30 min at 25°C using a REMI R4C centrifuge to evaluate their stability [21,22]. **"**The solid contents of the WPUUs were determined by following the ISO124-1997 standard method. A fixed amount of WPUU dispersion was placed in an aluminum cup and dried in a vacuum oven at 80°C until the weight of the solid contents was constant. The solid contents were then calculated using the following equation:

$$\text{Solid contents}(\%) = \frac{\text{A} - \text{B}}{\text{D}} \times 100$$

Where, B = mass of empty aluminium cup, D = mass of the cup and WPUC before drying, and A= mass of cup and WPUC after complete drying.**"**

5.3.3.2. DLS

Using a Zetasizer (Malvern, UK), the particle size distribution of the WPUU dispersion was measured by the DLS method. The WPUU dispersion samples were diluted to a concentration of 0.1 mL of the dispersion in 3 mL of distilled water

5.3.3.3. Electrolytic stability

The electrolytic stability of synthesized WPUU was analysed by mixing 10 mL of WPUU with 10 mL of distilled water and titrated with 2M NaCl until coagulation was appeared.

5.3.3.4. ATR-FTIR

ATR-FTIR spectroscopy was employed for the characterization of WPUU. Spectra were obtained within the range of 4000–400 cm^{-1} using a Bruker Tensor 11 spectrometer, which featured a diamond disk as the internal reflection element. Prior to each sample analysis, the spectrum of air was taken as a background. These ATR-FTIR measurements were utilized to confirm the formation of WPUU.

5.3.3.5. Chemical and solvent resistance

The chemical and solvent resistance of WPUU films was determined through ASTM-D543-06 standard method.

5.3.3.6. Mechanical properties

Tensile properties of the WPUU films were analysed using an universal testing machine (UTM) with a crosshead speed of 10 mm/min. The films with a length 80 mm and a width 10 mm were used for the analysis.

5.3.3.7. Morphology

The morphology of the WPUU films was performed on SEM. The surfaces were sprayed with gold for 60 s, and the surface morphology of film were characterized at 5 kV under high vacuum mode.

5.3.3.8. DSC

The Tg of the WPUU films was determined using DSC measurements conducted with TA Instruments (DSC 200 F3 Maia, NETZSCH-India). All DSC measurements were carried out according to the standard ISO11357:1-2023 method. The measurements were conducted in two cycles. The first cycle ranged from RT to -50°C, while the second cycle covered a temperature range of -50°C to 100°C with a heating rate of 10°C/min under a dry N_2 atmosphere.

5.3.3.9. TGA

The TGA of WPUU films with varying ratios was analyzed using a STA 449 F3 Jupiter analyzer from TA Instruments. The samples were subjected to heating from RT up to 700 °C at different heating rates (10°, 15°, and 20°C/min). The experiment was conducted with N_2 as the purge gas, and samples weighing less than 10 mg each were utilized for the test

5.3. Results and discussions

5.3.1. Physical characteristics of WPUU dispersions

The results of physical characterization of WPUU dispersion of varying weight percentage of OA are shown in **Table 5.2**. Solid contents of the synthesized WPUUs dispersions were found to be from 30.32% to 33.30%.

Increasing the amount of OA as a chain extender in PUU dispersion leads to a high percentage of solid content. Here, OA enhances the polymerization reaction efficiency and improves the polymer density in the dispersion, which results in the high solid content in the dispersion. All the WPUU dispersions physically appeared as milky white (shown in **Figure 5.2**). It is also clearly observed that the stability of all the synthesized dispersions (WPUU0 to WPUU1) was the same, as they did not show any phase separation for more than 9 months at usual RT conditions. It indicated the homogeneous formation of WPUU dispersions.

Table 5.2. Properties of the synthesized WPUU dispersions.

Properties	WPUU0	WPUU1	WPUU2	WPUU3
Appearance	Milky white	Milky white	Milky white	Milky white
Ave. particle size	130.9	129.5	123.6	109.6
PDI	0.242	0.276	0.187	0.274
Solid contains	30.32	30.82	32.02	33.32
Storage stability	>9 months	>9 months	>9 months	>9 months

Figure 5.2. Physical appearance of synthesized WPUU dispersions

5.3.2. DLS of WPUU dispersions

The particle size distribution of the synthesized WPUU dispersions was analyzed using the DLS method. **Figure 5.3** illustrates the particle size distribution of the WPUU dispersions at varying weight percentages of OA. The hydrodynamic diameter (Dh) of the WPUC dispersions was measured and found to be 130.9 nm for WPUU0, 129.5 nm for WPUU1, 123.6 nm for WPUU2, and 109.6 nm for WPUU3, respectively. Results showed that all the WPUU dispersions exhibit quite small particle sizes (d < 200 nm)[23] with narrow particle size distribution as PDI was less than 0.5. Such small particle sizes and narrow PDI resulted in the uniform and well-dispersed WPUU systems. It was noted that with increasing OA content in the WPUU dispersion, the particle size of the WPUU decreased from 130.9 to 109.6 nm. Here, the chain extender (OA) plays a crucial role in promoting the polymerization reaction and formation of longer polymer chains, which results in the formation of a high-cross-linking density and more compact polymer network.

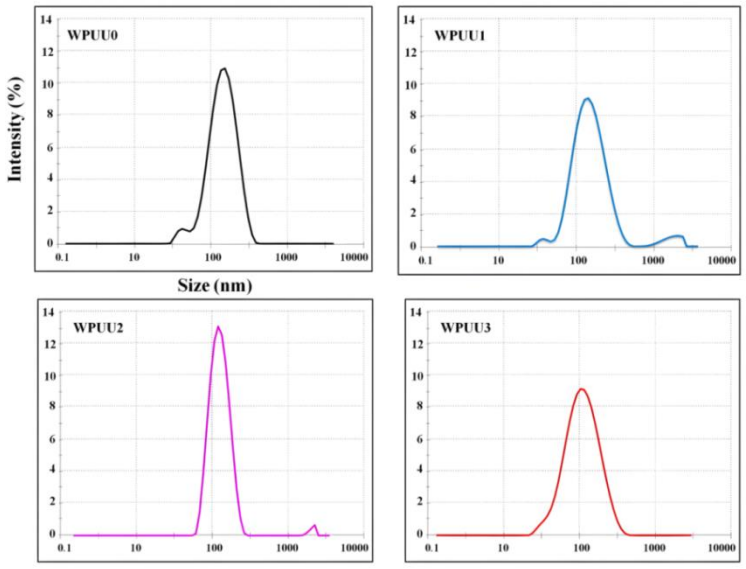

Figure 5.3. The particle size distribution of synthesized WPUUs

5.3.3. Electrolytic stability of WPUU dispersions

The addition of strong electrolytes is known to disrupt PUU dispersion by disturbing the double electric layers within the ionomer particles [24]. To assess the electrolytic stability of WPUU dispersion, a 2.0 M NaCl solution was introduced into the 10 mL of dispersion until the coagulation occurred. **Figure 5.4** shows the volume of NaCl solution required to coagulate the WPUU dispersion and it shows that as particle size of WPUU in dispersion decreases, the required volume of NaCl solution increases. This is because of the double electric layers increase with decrease in particle size and hence more volume of NaCl solution is required to coagulate the WPUU with smaller particle size.[24,25]

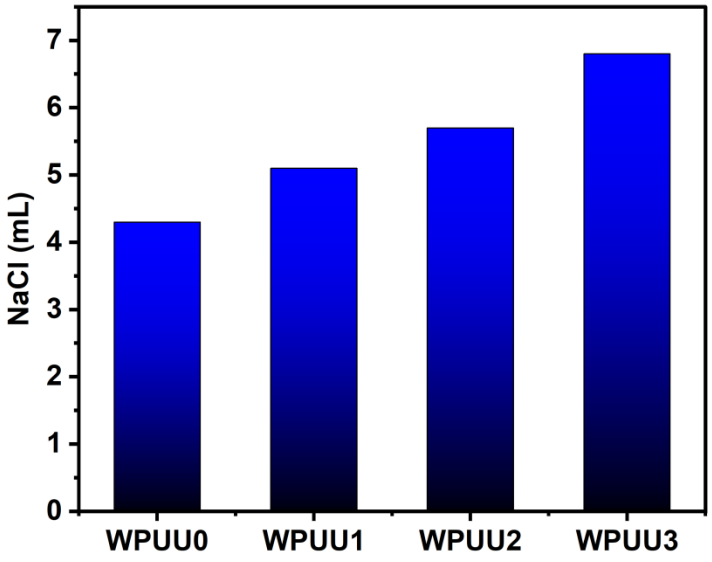

Figure 5.4. Electrolytic stability of WPUUs dispersion

5.3.4. ATR-FTIR of WPUU films

The ATR-FTIR Spectrum of four different WPUUs is shown in the **Figure 5.5**. The absence of the peak at 2270 cm^{-1}, identified as the stretching vibration band of NCO group, revealed a complete reaction of the NCO groups. The bands between 3200 and 3500 cm^{-1} correspond to the urethane and urea NH.

Hydrogen-bonding plays a very important role in WPUUs and significantly affects the properties of the material. ATR-FTIR spectroscopy can be used to investigate hydrogen-bonding in WPUUs and help understand the phase structure. In these WPUUs, the hydrogen bonds are mainly formed between NH bonds and the urethane/urea C=O group. As seen in **Figure 5.5**, a single stretching peak located around 3325 cm^{-1} corresponds to a hydrogen-bonded NH stretching vibration [23]. The hydrogen-bonded C=O groups of the urethane are observed at 1706 cm^{-1} [26]. The C=O stretch around 1706 cm^{-1} can be attributed to hydrogen-bonding in disordered regions, that is, urethane/urea linkages “dissolved” in soft segment

phases [27]. The stronger hydrogen-bonding in the ordered/crystalline regions of the urethane C=O groups occurs at a lower frequency, ranging from 1675 to 1706 cm^{-1}. This is not observed inWPUU0, indicating the amorphous nature of these WPUUs. The band at 1706 cm^{-1} is attributed to the H-bonded urethane C=O and a small shoulder at 1636 cm^{-1} corresponds to the urea C=O stretching.[28]

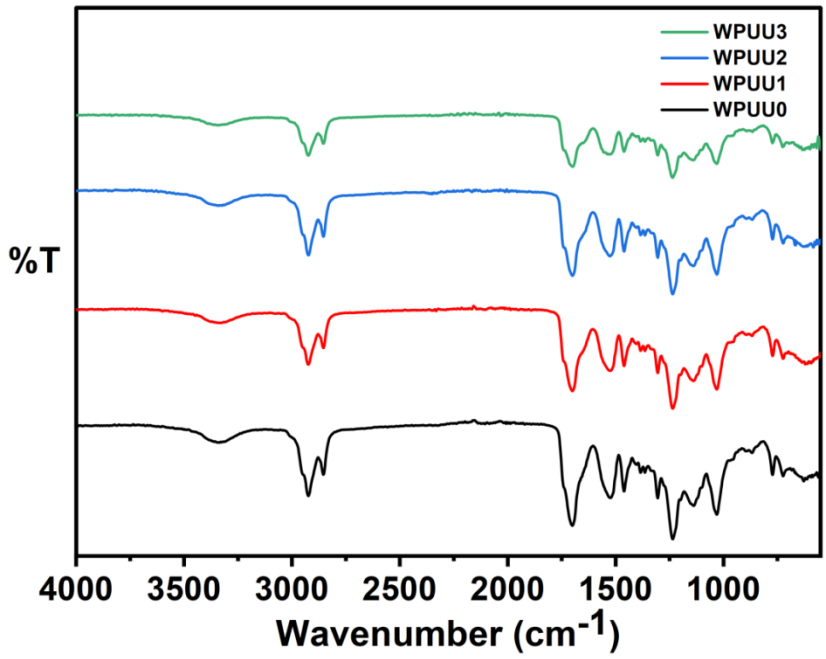

Figure 5.5. ATR-FTIR of synthesized WPUU films

5.3.5. Chemical resistance test of WPUU films

The chemical resistance of WPUU films was tested using acid, alkali, salt solutions, and different solvents. Results of this analysis were reported in **Table 5.3**. **"**The film samples about ~0.5 gm weight were immersed in corresponding medium for 48 hr at RT. After that, the samples were removed from the medium and wiped off smoothly with filter paper. The complete dry films were then weighed, and the % weight loss or weight gain was calculated using the following equations.

$$\%\text{weight gain and weight loss} = \frac{(W_1 - W)}{W} \times 100$$

Where W= weight of initial film and W_i= extracted films**"**

From the chemical resistance analysis, it was cleared that the increase OA amount from WPUUs, the water absorption was decreased and chemical resistance, acid and salt water resistances were increased. Due to the increased concentration of OA as a chain extender in PUU formulations enhances resistance to salts, acids, solvents, and water. The

long hydrophobic chains as well as existence of cross-linking present in OA impart greater hydrophobicity to the polymer, diminishing water absorption and degradation. Furthermore, the chemical structure of OA contributes to higher cross-linking density and polymer's chemical inertness, making it more resistant to acid and solvent attacks. The increase in hydrophobic nature of the film surface, the water absorption was decreased. The increase in solvent resistance with higher amount of OA in WPUU can be attributed to heightened concentrations leading to increased cross-linking density within the WPUU matrix, thereby hindering solvent penetration.[29] Furthermore, all the film samples were dissolved in alkali solution after 5 h of immersion and this is mainly because of the existence of ester linkages in the ionic soft segment which experienced hydrolysis in alkali media.

Table 5.3. Chemical and solvent resistance of WPUU films

Chemicals & solvents	WPUU0	WPUU1	WPUU2	WPUU3
3% H_2SO_4	+1.95	+1.74	+1.51	+0.25
3% HCl	+3.52	+3.21	+2.34	+1.46
3% NaOH	Soluble	Soluble	Soluble	Soluble
3% NaCl	+5.04	+4.31	+3.94	+2.34
Water	+20.3	+18.4	+15.2	+10.4
Acetone	-9.22	-8.02	-5.13	-2.43
Toluene	-8.23	-7.80	-7.20	-6.68
Xylene	-8.22	-7.92	-7.43	-6.90

(+) % Weight gain, (-) %Weight loss

5.3.6. Mechanical properties of WPUU films

The performance of materials is always presented in terms of their mechanical characteristics, such as tensile properties. These characteristics are important in order to predict or determine material ability, especially under extreme and critical conditions, which are directly connected with engineering performance. The load extension graph shown in **Figure 5.6** and **Table 5.4** summarizes their young's modulus, tensile strength, and elongation at break values. All sample behave as a elastomeric polymers with elongation at break values higher than 78.45 mm, which indicates that these sample can effectively sustain the stretch when stressed. For sample WPUU0 to WPUU3 improves the mechanical properties significantly. For example, the young's modulus and tensile strength increase from 98.40 to 155.14 N/mm^2 and 5.43 to 7.04 kgf respectively. The increase in Young's modulus and tensile strength with higher amounts of OA is primarily due to higher crosslinking density. OA, being a diamine, reacts with isocyanate groups during polymerization to form additional urea linkages, creating more crosslinking points in the polymer matrix. This denser network

restricts the mobility of polymer chains, making the material stiffer and improving its ability to resist deformation, which explains the increase in Young's modulus. Additionally, the tightly crosslinked structure enhances load transfer across the matrix, reducing weak points and enabling the material to withstand greater stress without failure, leading to improved tensile strength**.** This stronger network significantly enhances its ability to resist deformation under stress, ultimately leading to higher tensile strength. However, this increased crosslinking restricts polymer chain mobility, reducing the material's ability to stretch before breaking, which results in a decrease in elongation at break. The elongation at break decreased from 113.18 to 78.45 mm, as expected, when the amount of OA is increased from 0 to 1 wt%.

Table 5.4. Mechanical property of WPUU films

Sample	Tensile strength (kgf)	Elongation at break (mm)	Young's modulus (N/mm^2)
WPUU0	5.43± 0.08	113.18 ± 1.2	98.40 ± 0.3
WPUU1	5.69± 0.13	101.64 ± 2.3	103.91 ± 0.3
WPUU2	6.03 ± 0.20	95.33 ± 2.1	116.42 ± 0.5
WPUU3	7.04 ± 1.30	78.45 ± 2.3	155.14 ± 3.0

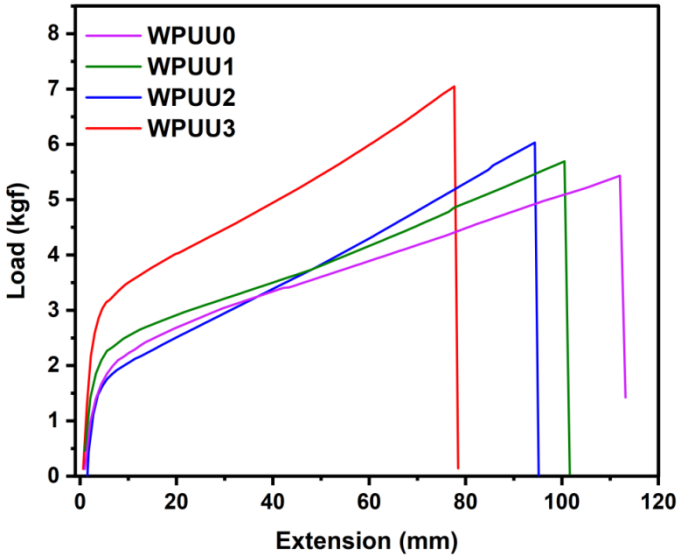

Figure 5.6. Load-Extension curve of WPUU films

5.3.7. Morphological of WPUU films

SEM study was carried out to evaluate the morphological appearances of the prepared WPUU Films. In **Figure 5.7**, the SEM images of all films showed a homogenous phase and smooth surface. This clearly suggested that the flexible and rigid segments were distributed properly, resulting in good phase mixing morphology in the resins.

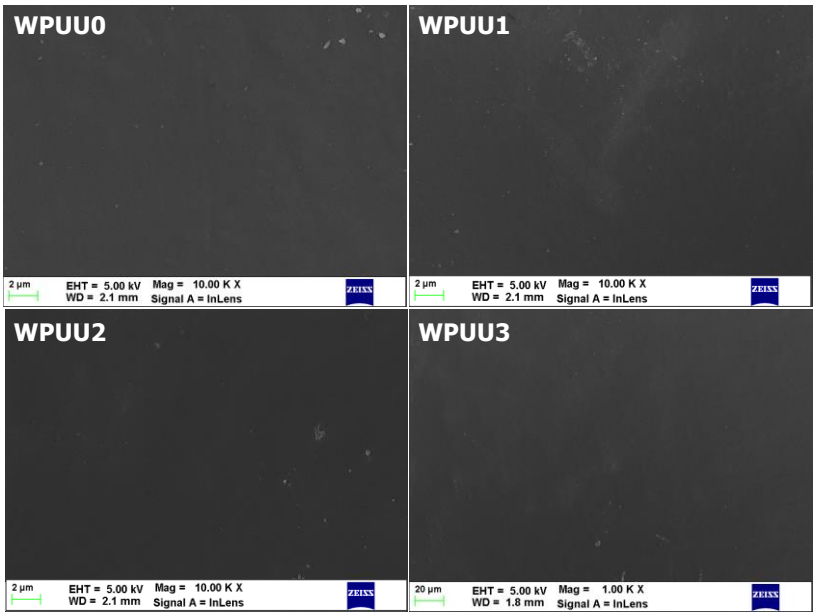

Figure 5.7. SEM images of WPUU films

5.3.8. Thermal behavior of WPUU films

5.3.8.1. DSC

DSC thermograms of WPUU films are shown in **Figure 5.8**. The peaks from the second heating DSC curves were taken to establish the Tg values of the WPUU films. The Tg, which measures the mobility of a chain segment and assesses a polymer's thermal behavior. The Tg values of the WPUU polymeric films are 36.8°C, 39.4°C, 52°C, and 57.4°C for WPUU0, WPUU1, WPUU2, and WPUU3, respectively.

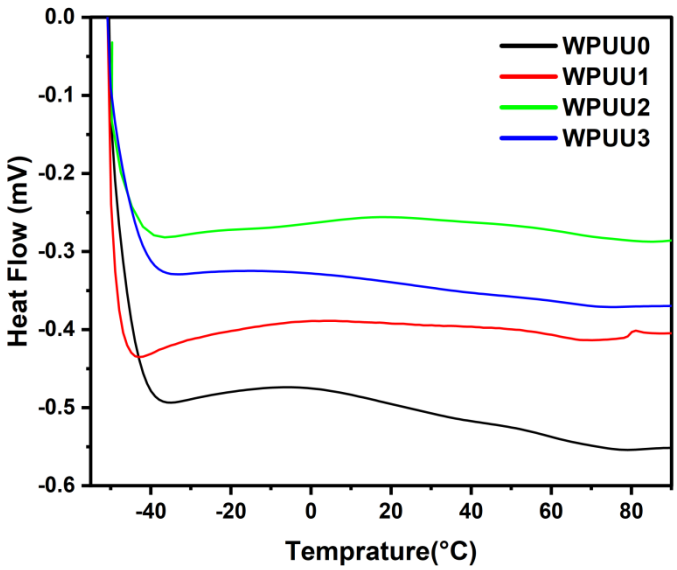

Figure 5.8. DSC thermograph of WPUU films

As OA content rises, more amine groups are available to react with isocyanate groups during the curing process, leading to the formation of additional urea linkages. These linkages act as

crosslinks, significantly increasing the crosslink density of the polymer network. A higher crosslink density restricts the mobility of the polymer chains, as the network becomes more rigid and interconnected. Tg represents the temperature at which polymer chains gain sufficient mobility to transition from a rigid to a rubbery state. When chain mobility is limited due to dense crosslinking, a higher temperature (Tg) is required for this transition.

5.3.8.2 TGA

The thermal properties of WPUU polymers mainly depended on the structure of polyol (soft segment) and isocyanate (hard segment). The TG curve of the WPUU films at different heating rates (10, 15, and 20℃/min) and their derivative plots are presented in **Figure 9**. Generally, PU films exhibit low thermal stability, mainly due to the presence of labile urethane bonds. PU films tend to decompose at temperatures below 250℃, depending on the types of isocyanates and polyols used during synthesis [30]. Upon analyzing the thermograms, it is seen that all the WPUU films initiated degrading above 200℃.

The decomposition process up to 350℃ can be attributed to the urethane bonds breaking, accompanied by the release of carbon dioxide [31,32]. Additionally, the range between 350° and 500°C temperature primarily corresponds to the degradation of the long alkyl chains present in the polyol segments. Also, thermal-oxidative breakdown of the WPUU films takes place at temperatures more than 500 ℃. The increasing amount of OA in the formation of WPUU films enhances their thermal stability. This is because the urea groups can form extensive hydrogen bonds with adjacent polymer chains, which increases the overall stability of the material. These hydrogen bonds require more thermal energy to break, thereby enhancing thermal stability. The improvement in stability in the WPUU films is clearly observed by examining the T10, T50, and T95 values, which showed the 10%, 50%, and 95% weight loss of WPUU films at different heating rates, respectively (displayed in **Tables 5.5, 5.6, and 5.7**). The char residue of WPUU0 to WPUU3 films undergoes complete degradation at 700℃.

The degradation of WPUU films occurs in four stages. In the first stage, the breakdown of urethane bonds (NH-CO-O) leads to the formation of primary amines and carbon dioxide, resulting in a small weight loss compared to subsequent stages. During the second stage, the breaking down of urea bonds (NH-CO-NH) along with the remaining urethane bonds leads to the formation of secondary amines, isocyanates, and other volatile products. In the third stage, the soft segments, often composed of polyols, degrade into various volatile compounds, such as aldehydes, ketones, and hydrocarbons. The final stage of degradation involves the oxidative decomposition of the remaining char residue.

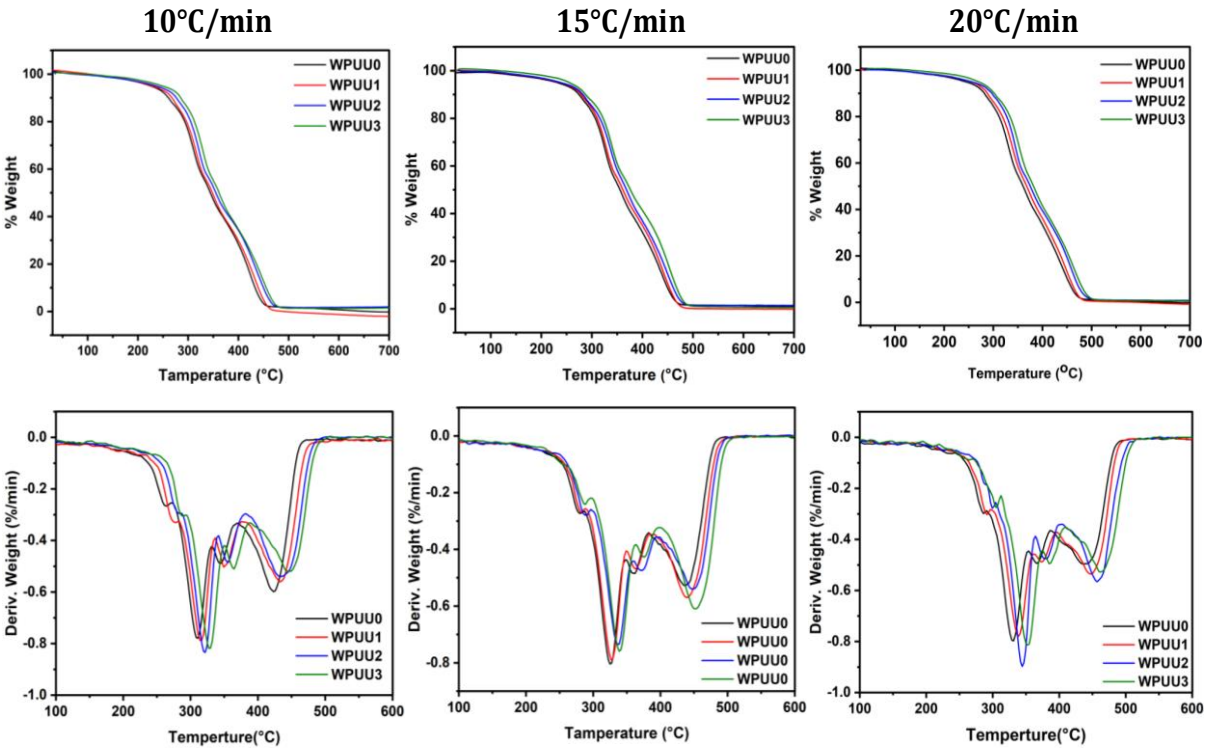

Figure 5.9. TGA curves and Derivative thermograms for the WPUU films taken at various heating rates

The Kissinger method was used to figure out the activation energy (Ea) parameters for the four different stages of the thermal decomposition process of WPUU films. This involved utilizing the following equation to calculate the activation energy values [33]:

$$\ln\left(\frac{\beta}{Tp^2}\right) = -\frac{Ea}{RTp} + \{\ln\frac{AR}{Ea} + \ln[n(1-\alpha_P)^{n-1}]\}$$

Here, the heating rate=β, the maximum temperature related to the maximum degradation=Tp, the pre-exponential factor=A, the activation energy=Ea, the maximum conversion=α_p, the order of the reaction=n, and the gas constant=R are represented. The activation energy can be examined from the slope (=E_a/R) of a linear plot of ln(β/Tp^2) vs. 1/Tp.

The Ea measures for the WPUU films were calculated and are provided in **Table 5.8 & Table 5.9**, and their corresponding Kissinger plots (**Figure 5.10**) at four different degradation stages were presented. The kinetic parameters of films changed with the incorporation of OA. It was observed that the Ea of the WPUU film degradation process increased as the amount of OA increased. Increasing the amount of OA in WPUU films raises the activation energy primarily due to higher crosslink density. OA furnishes more amine groups that react with isocyanate groups during curing, forming more urea linkages and creating a denser, tightly interconnected polymer network. This increased crosslink density

restricts the mobility of PU chains, making it more difficult to undergo deformation. As a result, more energy is required to diminish the rigidity and break bonds within the structure, leading to a higher activation energy. This denser network not only reduces chain flexibility but also enhances the thermal stability of the material, further contributing to the increased energy requirement.

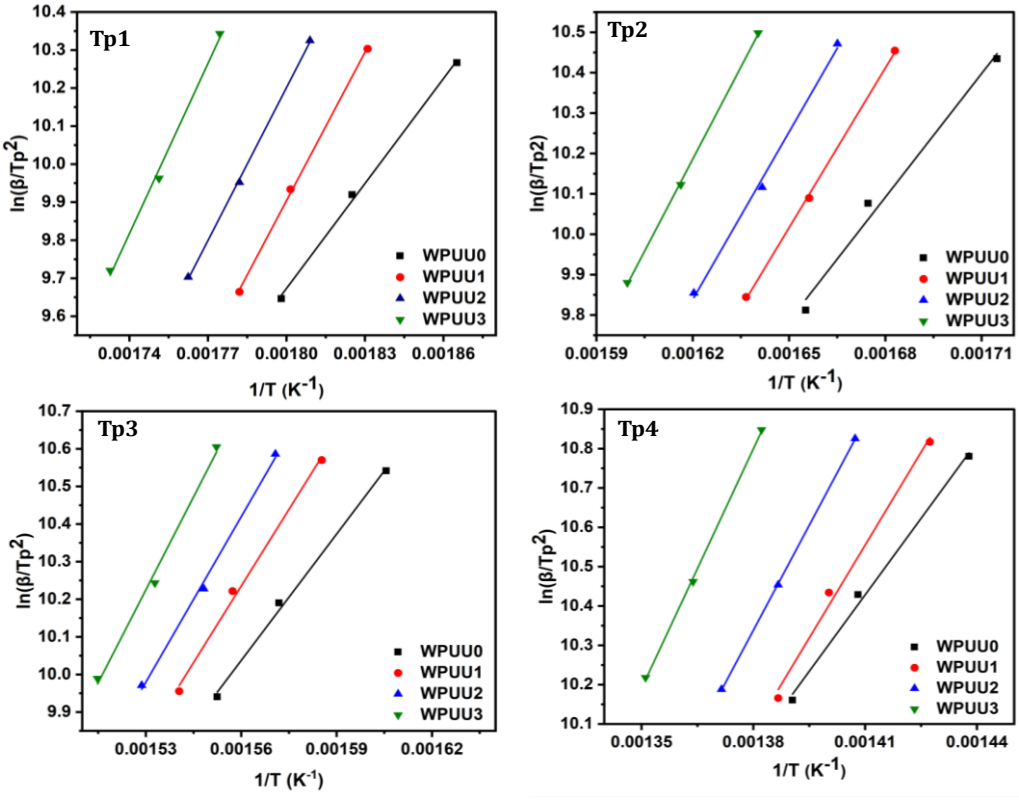

Figure 5.10. Kissinger plot of WPUU films at two different stages of the degradation

Table 5. Thermal properties of WPUU films at a heating rate of 10°C/min

Sample	Temperature (°C) at % weight loss 10/min			Char residue (%) at 700°C
	10%	50%	95%	
WPUU0	258	343	443	00
WPUU1	266	346	448	00
WPUU2	274	354	459	00
WPUU3	284	359	464	00

Table 6. Thermal properties of WPUU films at a heating rate of 15°C/min

Sample	Temperature (°C) at % weight loss 15/min			Char residue (%) at 700°C
	10%	50%	95%	
WPUU0	272	354	452	00
WPUU1	276	361	461	00
WPUU2	278	366	468	00
WPUU3	286	376	473	00

Table 7. Thermal properties of WPUU films at a heating rate of 20°C/min

Sample	Temperature (°C) at % weight loss 20/min			Char residue (%) at 700°C
	10%	50%	95%	
WPUU0	281	358	461	00
WPUU1	286	366	466	00
WPUU2	296	374	476	00
WPUU3	299	379	482	00

Table 8. Activation energy value of WPUU films

Sample	Degradation (Tp1)			Degradation(Tp2)		
	Slope	R^2	E_a (kJ/mol)	Slope	R^2	E_a (kJ/mol)
WPUU0	9198.15	0.99817	76.47	10209.95	0.98747	84.88
WPUU1	13013.09	0.99928	108.19	13187.98	0.99937	109.64
WPUU2	13400.54	0.99949	111.41	13820.01	0.99644	114.89
WPUU3	14912.91	0.99586	123.98	15193.74	0.99966	126.32

Table 9. Activation energy value of WPUU films

Sample	Degradation (Tp3)			Degradation(Tp4)		
	Slope	R^2	E_a (kJ/mol)	Slope	R^2	E_a (kJ/mol)
WPUU0	11201.62	0.99677	93.13	12950.68	0.99507	107.67
WPUU1	13573.36	0.99558	112.89	15738.25	0.99230	130.64
WPUU2	14661.45	0.99709	121.89	17794.78	0.99992	147.94
WPUU3	16483.87	0.99372	137.04	20285.10	0.99936	168.65

5.4. Reference

(1) Zhang, C.; Liang, H.; Liang, D.; Lin, Z.; Chen, Q.; Feng, P.; Wang, Q. Renewable castor-oil-based waterborne polyurethane networks: simultaneously showing high strength, self-healing, processability and tunable multishape memory. *Angewandte Chemie International Edition* **2021**, *60* (8), 4289–4299. https://doi.org/10.1002/anie.202014299.

(2) Dai, M.; Zhai, Y.; Zhang, Y. A Green approach to preparing hydrophobic, electrically conductive textiles based on waterborne polyurethane for electromagnetic interference shielding with low reflectivity. *Chemical Engineering Journal* **2021**, *421*, 127749. https://doi.org/10.1016/j.cej.2020.127749.

(3) Santamaria-Echart, A.; Fernandes, I.; Barreiro, F.; Corcuera, M. A.; Eceiza, A. Advances in waterborne polyurethane and polyurethane-urea dispersions and their eco-friendly derivatives: a review. *Polymers* **2021**, *13* (3), 409. https://doi.org/10.3390/polym13030409.

(4) Zhou, W.; Gong, X.; Li, Y.; Si, Y.; Zhang, S.; Yu, J.; Ding, B. Environmentally friendly waterborne polyurethane nanofibrous membranes by emulsion electrospinning for waterproof and breathable textiles. *Chemical Engineering Journal* **2022**, *427*, 130925. https://doi.org/10.1016/j.cej.2021.130925.

(5) Dall Agnol, L.; Dias, F. T. G.; Ornaghi, H. L.; Sangermano, M.; Bianchi, O. UV-curable waterborne polyurethane coatings: a state-of-the-art and recent advances review. *Progress in Organic Coatings* **2021**, *154*, 106156. https://doi.org/10.1016/j.porgcoat.2021.106156.

(6) Liang, Z.; Zhu, J.; Li, F.; Wu, Z.; Liu, Y.; Xiong, D. Synthesis and properties of self-crosslinking waterborne polyurethane with side chain for water-based varnish. *Progress in Organic Coatings* **2021**, *150*, 105972. https://doi.org/10.1016/j.porgcoat.2020.105972.

(7) Noble, K.-L. Waterborne polyurethanes. *Progress in Organic Coatings* **1997**, *32* (1), 131–136. https://doi.org/10.1016/S0300-9440(97)00071-4.

(8) Sardon, H.; Irusta, L.; Fernández-Berridi, M. J.; Luna, J.; Lansalot, M.; Bourgeat-Lami, E. Waterborne polyurethane dispersions obtained by the acetone process: a study of colloidal features. *Journal of Applied Polymer Science* **2011**, *120* (4), 2054–2062. https://doi.org/10.1002/app.33308.

(9) Subramani, S.; Park, Y.-J.; Lee, Y.-S.; Kim, J.-H. New Development of polyurethane dispersion derived from blocked aromatic diisocyanate. *Progress in Organic Coatings* **2003**, *48* (1), 71–79. https://doi.org/10.1016/S0300-9440(03)00118-8.

(10) Patel, R. H.; Shah, M. D.; Patel, H. B. Synthesis and characterization of structurally modified polyurethanes based on castor oil and phosphorus-containing polyol for flame-retardant coatings. *International Journal of Polymer Analysis and Characterization* **2011**, *16* (2), 107–117. https://doi.org/10.1080/1023666X.2011. 541108.

(11) Ionescu, M.; Radojčić, D.; Wan, X.; Shrestha, M. L.; Petrović, Z. S.; Upshaw, T. A. Highly functional polyols from castor oil for rigid polyurethanes. *European Polymer Journal* **2016**, *84*, 736–749. https://doi.org/10.1016/j.eurpolymj.2016.06.006.

(12) Tu, Y.-C.; Kiatsimkul, P.; Suppes, G.; Hsieh, F.-H. Physical properties of water-blown rigid polyurethane foams from vegetable oil-based polyols. *Journal of Applied Polymer Science* **2007**, *105* (2), 453–459. https://doi.org/10.1002/app.26060.

(13) Mubofu, E. B. Castor oil as a potential renewable resource for the production of functional materials. *Sustain Chem Process* **2016**, *4* (1), 11. https://doi.org/10.1186 /s40508-016-0055-8.

(14) Madbouly, S. A.; Xia, Y.; Kessler, M. R. Rheological behavior of environmentally friendly castor oil-based waterborne polyurethane dispersions. *Macromolecules* **2013**, *46* (11), 4606–4616. https://doi.org/10.1021/ma400200y.

(15) Ji, X.; Zhou, Y.; Zhang, B.; Hou, C.; Ma, G. Polydimethylsiloxane and castor oil comodified waterborne polyurethane. *International Scholarly Research Notices* **2013**, *2013* (1), 284683. https://doi.org/10.1155/2013/284683.

(16) Špírková, M.; Pavličević, J.; Aguilar Costumbre, Y.; Hodan, J.; Krejčíková, S.; Brožová, L. Novel waterborne poly(urethane-urea)/silica nanocomposites. *Polymer Composites* **2020**, *41* (10), 4031–4042. https://doi.org/10.1002/pc.25690.

(17) Lu, Y.; Tighzert, L.; Dole, P.; Erre, D. Preparation and properties of starch thermoplastics modified with waterborne polyurethane from renewable resources. *Polymer* **2005**, *46* (23), 9863–9870. https://doi.org/10.1016/j.polymer.2005.08.026.

(18) Jin-qing, Q. U.; Huan-qin, C. Studies on syntheses and properties of waterborne polyurethane resin from CO. 林产化学与工业 **2004**, *24* (3), 78–82.

(19) Gurunathan, T.; Arukula, R.; Suk Chung, J.; Rao, C. R. K. Development of environmental friendly castor oil-based waterborne polyurethane dispersions with

polyaniline. *Polymers for Advanced Technologies* **2016**, *27* (11), 1535–1540. https://doi.org/10.1002/pat.3797.

(20) Parth KaPatel; Rasmika Patel. Flame retardant waterborne polyurethanes: synthesis, characterization, and evaluation of different properties. *Biointerface Research in Applied Chemistry* **2021**, *12* (3), 3198–3214. https://doi.org/10.33263/BRIAC123. 31983214.

(21) Li, M.; Qiang, X.; Xu, W.; Zhang, H. Synthesis, characterization and application of afc-based waterborne polyurethane. *Progress in Organic Coatings* **2015**, *84*, 35–41. https://doi.org/10.1016/j.porgcoat.2015.02.009.

(22) Ganvit, V. M.; Bhandari, P. D.; Kunjadiya, A.; Mansuri, J.; Bambhaniya, S. B.; Mandot, A. A.; Sharma, R. K. Waterborne polyurethane polymer dispersions using castor oil and curcumin as bioresources: synthesis, characterization, and antibacterial textile applications. *Journal of Applied Polymer Science* **2024**, *141* (24), e55509. https://doi.org/10.1002 /app.55509.

(23) Srichatrapimuk, V. W.; Cooper, S. L. Infrared thermal analysis of polyurethane block polymers. *Journal of Macromolecular Science, Part B* **1978**, *15* (2), 267–311. https://doi.org/10.1080/00222347808212599.

(24) Gaddam, S. K.; Palanisamy, A. Effect of counterion on the properties of anionic waterborne polyurethane dispersions developed from cottonseed oil based polyol. *Journal of Polymer Research* **2018**, *25* (8), 186. https://doi.org/10.1007/s10965-018-1580-9.

(25) Gaddam, S. K.; Palanisamy, A. Anionic waterborne polyurethane dispersions from maleated cotton seed oil polyol carrying ionisable groups. *Colloid and Polymer Science* **2016**, *294* (2), 347–355. https://doi.org/10.1007/s00396-015-3787-1.

(26) Pollack, S. K.; Shen, D. Y.; Hsu, S. L.; Wang, Q.; Stidham, H. D. *Infrared and x-ray diffraction studies of a semirigid polyurethane*. ACS Publications. https://doi.org/ 10.1021/ma00192a007.

(27) Teo, L.-S.; Chen, C.-Y.; Kuo, J.-F. Fourier transform infrared spectroscopy study on effects of temperature on hydrogen bonding in amine-containing polyurethanes and poly(urethane−urea)s. *Macromolecules* **1997**, *30* (6), 1793–1799. https://doi.org/10. 1021/ma961035f.

(28) Xia, Y.; Larock, R. C. soybean oil–isosorbide-based waterborne polyurethane–urea dispersions. *ChemSusChem* **2011**, *4* (3), 386–391. https://doi.org/10.1002/cssc. 201000411.

(29) Li, X.; Hu, J.; Sun, D.; Zhang, Y. Nanosilica reinforced waterborne siloxane-polyurethane nanocomposites prepared via “click” coupling. *Journal of Coating Technology Research* **2014**, *11* (4), 517–531.https://doi.org/10.1007/s11998-013-95636.

(30) Xia, Y.; Larock, R. C. Preparation and properties of aqueous castor oil-based polyurethane–silica nanocomposite dispersions through a sol–gel process. *Macromolecular Rapid Communications* **2011**, *32* (17), 1331–1337. https://doi.org/10. 1002/marc.201100203.

(31) Petrović, Z. S.; Yang, L.; Zlatanić, A.; Zhang, W.; Javni, I. Network structure and properties of polyurethanes from soybean oil. *Journal of Applied Polymer Science* **2007**, *105* (5), 2717–2727. https://doi.org/10.1002/app.26346.

(32) Ganvit, V. M.; Patel, V.; Patel, M.; Dharva, A.; Sharma, R. K. Synthesis, physicochemical and thermal properties of urethane-modified polyesteramide films using mahua and castor oil as sustainable resources. *Journal of Applied Polymer Science* **2024**, *141* (5), e54872. https://doi.org/10.1002/app.54872.

(33) Li, J.; Tong, L.; Fang, Z.; Gu, A.; Xu, Z. Thermal degradation behavior of multi-walled carbon nanotubes/polyamide 6 composites. *Polymer Degradation and Stability* **2006**, *91* (9), 2046–2052. https://doi.org/10.1016/j.polymdegradstab.2006.02.001.